

## The Effects of Hydrogen on Mechanical Properties of Ni-base Alloys under the Static and Cyclic Loading.

**Alexander Balitskii\*, Lyubomir Ivaskevich, Volodimir Mochulskiy.**

Department of Hydrogen Resistance of Materials Karpenko Physico-Mechanical Institute,  
5 Naukova str., Lviv, 79601, Ukraine  
\* balitski@ipm.lviv.ua

**Abstract** The effect hydrogen on short-term strength, low-cycle durability and plane-stress fracture toughness of 04Cr16Ni56 and 05Cr19Ni55 alloys at pressure up to 35 MPa and temperature 293...1073 K was investigated. The modes of hydrogen action for which the mechanical properties of alloys are minimum were established: hydrogen pressure above 10 MPa (non-hydrogenated specimens of 04Cr16Ni56 alloy) and above 35 MPa (hydrogenated specimens of 05Cr19Ni55 alloy, hydrogen concentration  $C_H = 19$  wppm). The plane-strain state conditions and, correspondingly, the conditions of the evaluation of plane-strain fracture toughness ( $K_{Ic}$ ) were fulfilled on compact tension specimens of 04Cr16Ni56 with a thickness of 20 mm at hydrogen pressure above 10 MPa in the temperature range 293...473 K. Plane-stress fracture toughness  $K_c$  of 05Cr19Ni55 alloys was decreased at 293 K from  $116 \text{ MPa}\cdot\text{m}^{1/2}$  in helium to  $78 \text{ MPa}\cdot\text{m}^{1/2}$  in hydrogen under the pressure 30 MPa and to  $68 \text{ MPa}\cdot\text{m}^{1/2}$  in hydrogen under the pressure 30 MPa after preliminary high-temperature hydrogenation (with hydrogen concentration  $C_H = 19$  wppm).

**Keywords** Hydrogen embrittlement, Fracture toughness, Alloy

---

### 1. Introduction

The production of turbine equipment requires a wide usage of dispersive hardened heat-resistant Fe-Ni alloys. In these products heat-resistant alloys are exploited at high temperatures in the contact with high-pressure hydrogen containing gas mixtures. Therefore one of the most important requirements for such alloys is their resistance to hydrogen degradation. In other words their ability to keep high level of mechanical properties under the action of hydrogen in wide range of exploitation parameters. At the same time, age-hardening alloys are known to be rather sensitive to hydrogen embrittlement [1-3].

The serviceability of structures in hydrogen is, as a rule, estimated according to the results of testing at room temperature [4-7]. This is explained by maximum sensitivity of steels and alloys to hydrogen degradation and complexity of experiments at elevated temperatures. However, the operating conditions of the equipment for hydrogen power engineering include static and cyclic loading of the products in hydrogen in fairly broad temperature ranges [7, 8], whereas the available literature data on the temperature dependences of mechanical properties in hydrogen are quite poor and ambiguous. In most cases, the influence of gaseous hydrogen on mechanical properties weakens as temperature increases and, according to the data presented in [6], the upper temperature of embrittlement under the analyzed conditions was equal to 573 K. At the same time, we reveal a significant decrease in the plasticity of heat-resistant nickel alloys in hydrogen under a pressure of 35 MPa at temperature 1073 K [3, 7, 9].

In what follows, we study the influence of high-pressure gaseous hydrogen on short-term strength, low-cycle durability, and static crack resistance of nickel based alloys in the temperature range 293-1073 K.

### 2. Materials and Experimental Procedure

Two types of dispersion-hardened alloys were investigated: 04Cr16Ni56 and 05Cr19Ni55. Alloying

with niobium, vanadium, titanium, aluminum and boron leads to the formation of carbide TiC, borides  $Me_3B_2$ , and intermetallics  $Ni_3(Al,Ti,Nb)$  in the amounts of to 8 % for 05Cr19Ni55 alloy and up to 15...17 % for 04Cr16Ni56 alloy, which substantially increases their high-temperature strength [8] and significantly influences the sensitivity to the action of hydrogen [3, 9]. Heat treatment regimes and the mechanical properties of alloys (Table 1) in helium and in hydrogen under a pressure of 35 MPa after preliminary hydrogenation to hydrogen content of 19 wppm (05Cr19Ni55 alloy) and 20 wppm (04Cr16Ni56 alloy). After heat treatment, the grain size was 40...60  $\mu$ , and the particle size of the intermetallic  $\gamma'$ -phase was 320...500  $\text{\AA}$ .

Table 1. Chemical Composition, Modes of Thermal Treatment and Mechanical Properties of Alloys in Helium/Hydrogen (35 MPa) at Room Temperature

Alloy	Thermal Treatment		Mechanical Properties					
	Solution treatment	Mode of aging	$\sigma_u$ , MPa	$\sigma_y$ , MPa	$\delta$ , %	$\psi$ , %	Number of cycles to fracture, bending strain 1.6 %	$K_c$ , MPa·m <sup>1/2</sup>
<b>04Cr16Ni56</b> (C-0.04; Si-0.12; Cr-16.4; Mo-5.24; V-0.35; Nb-5.19; Ti-0.58; Al-1.0; Fe-15.14; Cu-0.49; Ni-bal)	1373K, 1 h	1023 K, 16 h + 923 K, 10 h	<u>1320</u> 880	<u>840</u> 750	<u>34</u> 4	<u>48</u> 12	<u>3205</u> 54	<u>134</u> 52
<b>05Cr19Ni55</b> (C-0.05; Si-0.23; Cr-19.0; Mo-8.87; Nb-1.73; I-1.49; Fe-12.0; Cu-0.02; Ni-bal)	1323K, 1 h	1000 K, 15 h + 923 K, 10 h	<u>1080</u> 970	<u>650</u> 660	<u>35</u> 7	<u>38</u> 21	<u>2560</u> 199	<u>116</u> 68

Static tensile tests with recorded “stress-strain” curves were carried out on standard five-fold cylindrical specimens using displacement rate  $V = 0.1$  mm/min. During the test the specimens were positioned into the chamber specially designed for high-temperature tests at 293...1093 K temperature range under 0.1...30 MPa hydrogen pressure. Specimens were tested in temperature range 293...1073 K under 30 MPa of hydrogen pressure and, as a comparison, in helium. The low-cycle durability for pure strain-controlled sign-preserving bending was investigated under pressures of 30 MPa for the strain amplitudes  $\varepsilon = 1.6\%$  and loading frequency of 0.5 Hz on polished plane specimens with a working part size 3 x 6 x 20 mm. Stress intensity factor under static loading  $K_c$  was computed either for the maximum force  $F_c$  in the "F-V" linear diagram or for the force  $F_Q$  determined by using the 5% secant for nonlinear diagrams. Rectangular compact specimens 50 x 60 x 20 mm in size were tested for eccentric tension in a high-pressure chamber under pressures of 0.4-30 MPa at strain rate of 0.1 mm/min. The values of  $K_c$  can be calculated from the Srawley-Gross formula [10].

To determine the indicated mechanical characteristics in hydrogen, the working chambers were preliminarily evacuated, blown-out with hydrogen, again evacuated, and filled up with hydrogen to a given pressure. At high temperatures, the specimens were held under the testing conditions for 30 min until the attainment of thermal equilibrium.

Earlier we established that, at some region of hydrogen pressure and strain rate exists a maximum

influence of hydrogen on the plasticity, low-cycle fatigue life, and static and cyclic crack resistance of martensitic steels and high nickel alloys [3, 7, 9]. In short-term tension, austenitic dispersion-hardened steels are substantially embrittled by hydrogen only after preliminary hydrogenation at elevated temperatures when its content becomes greater than 12 wppm [3, 7]. This is why we held a part of the specimens for 10 h in a hydrogen atmosphere under 623 K and 35 MPa. These regimes provide the hydrogenation of specimens to hydrogen contents of 19 wppm (05Cr19Ni55 alloy) and 20 wppm (04Cr16Ni56 alloy). Hydrogenated and non-hydrogenated specimens were tested in helium and hydrogen under different pressures.

Hydrogen concentration ( $C_H$ ) was determined with a LECO TCH 600 instrument [11] with precise 0.1 ppm (3 samples for point).

## 2. Hydrogen Pressure Influence on the Mechanical Properties.

It is known from the literature for almost materials and testing methods the influence of hydrogen increases proportionally to the square root of pressure [1, 4, 6, 12]. The pressure range for which this dependence is valid is studied insufficiently. In the process of short-term static tension, the properties of carbon steels deteriorate only in the range 0-10 MPa. Embrittlement of specimens made of Inconel-718 alloy begins only when the pressure reaches 10 MPa and increases up to 70 MPa [12]. Hydrogen influence on plasticity of steels and many other materials increases in the entire pressure range (0-70 MPa) [1, 3, 6, 12].

In the case of 04Cr16Ni56 alloy the dependence of low-cycle durability ( $N$ ), the plasticity parameters ( $\delta$  and  $\psi$ ) (Fig.1a) and plane-stress fracture toughness ( $K_{Ic}$ ) (Fig.2, curves 3, 4) on the hydrogen pressure consists of two regions. In the first region (low pressures), parameters  $N$ ,  $\delta$ ,  $\psi$  and  $K_{Ic}$  drops abruptly, and in the second, the negative influence of hydrogen is practically independent of pressure (figs. 1, 2). This means that there exists a pressure which cause the limiting degradation of materials properties. An additional effect of preliminary dissolved hydrogen ( $C_H = 20$  wppm) on the properties of 04Cr16Ni56 alloy was manifested at hydrogen environment pressure less than 10 MPa. The parameters of loading and the modes of hydrogen action for which the mechanical characteristics of the investigated alloys are minimum at 293 K can be formulated as follows: –the strain rate  $V_{def} = 0,1$  mm/min ( $6.7 \cdot 10^{-5}$  s $^{-1}$ ) at short-term static tension and static crack propagation; – the frequency and amplitude of bending under the conditions of low-cycle fatigue are  $\nu = 0, 5$  Hz and  $\epsilon = 1.6\%$  respectively, and the pressure of hydrogen must be higher than 10 MPa.

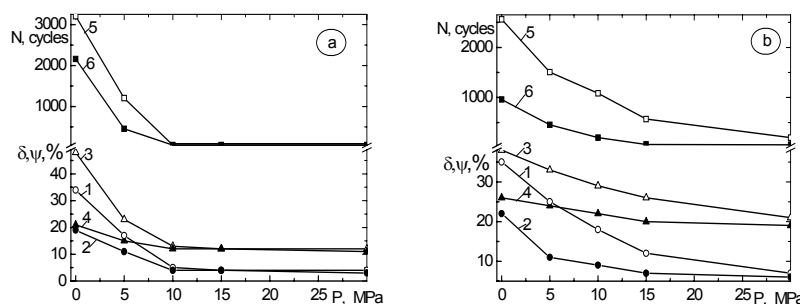


Figure 1. The relative elongation  $\delta$  (1, 2), reduction of area  $\psi$  (3, 4) ( $V = 0,1$  mm/min.) and number cycles to failure  $N$  (5, 6) ( $\epsilon = 1,6\%$ ) specimens of 04Cr16Ni56 (a) and 05Cr19Ni55 (b) alloys versus hydrogen pressure  $P$  at 293 K: 1, 3, 5 – non-hydrogenated specimens; 2, 4, 6 – hydrogenated specimens.

In the case of 05Cr19Ni55 alloy the low-cycle durability  $N$ , plasticity parameters  $\delta$  and  $\psi$  (Fig.2b, curves 1, 3, 5) and plane-stress fracture toughness  $K_{Ic}$  (Fig.3, curve 1) decrease in whole hydrogen pressure range. Preliminary dissolved hydrogen ( $C_H = 19$  wppm) leads to a considerable additional decrease in the properties of this alloy (Fig.2b, curves 2, 4, 6; Fig.3, curve 2). Maximum hydrogen effect achieved on hydrogenated specimens at hydrogen pressure above 10 MPa.

Thus, to estimate the serviceability of alloy 04Cr16Ni56 it suffices to test the specimens in gaseous hydrogen, while for alloy 05Cr19Ni55 there is a need for preliminary hydrogenation.

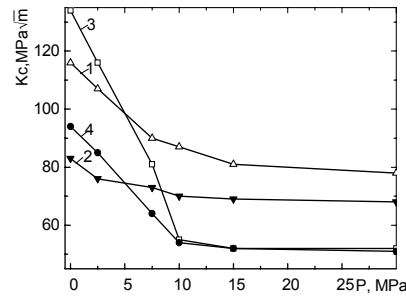


Figure 2. Fracture toughness  $K_c$  of 05Cr19Ni55 (1, 2) and 04Cr16Ni56 (3, 4) alloys versus hydrogen pressure  $P$  at 293 K: 1, 3 – non-hydrogenated specimens; 2, 4 – hydrogenated specimens.

Hydrogen decreases the stress intensity factor  $K_c$  and affects the fracture morphology. Under the conditions of maximum hydrogen embrittlement, the load-displacement diagrams become linear with sharp maxima (as functions of the load) (Fig.3a) and correspond to type I [10]. The fracture surfaces of the specimens are intergranular with cleavage facets typical of brittle fracture (Fig.4b), when in helium the honeycomb relief with ductile intergranular fracture portions is prevailed (Fig.4a). The values of  $K_c$  can be regarded as equal to  $K_{Ic}$ , i.e., they satisfy the condition  $l, b > 2.5(K_c^H / \sigma_{0.2}^H)^2$ , where  $l$  is the crack length and  $b$  is the thickness of the specimen [10]. The indicated condition is satisfied at room temperature for alloy 04Cr16Ni56 under pressures of hydrogen higher than 10 MPa for which  $K_{Ic}$  is equal to 52 MPa·m<sup>1/2</sup>. The plane-strain state conditions were not fulfilled for the specimens made of alloy 05Cr19Ni55.

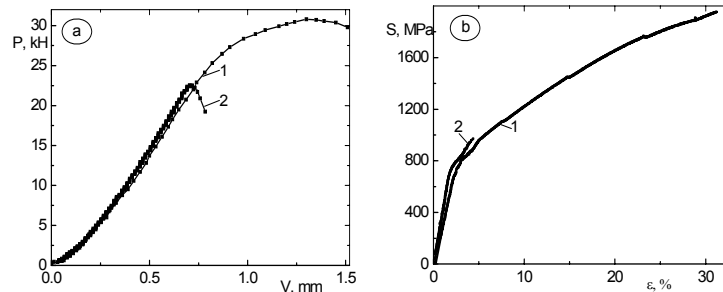


Figure 3. Diagrams “loading – crack opening displacement” (a) and true “stress-strain” diagram (b) of 04Cr16Ni56 alloys in helium (1) and hydrogen (2) under pressure 30 MPa at 293 K.

Hydrogen produced changes in true stress diagrams of both alloys in wide pressure and temperature range: essentially decrease failure stress and deformation of specimens (Fig.3b).

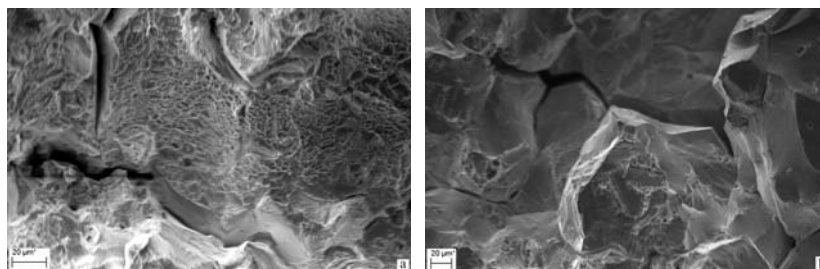


Figure 4. Fracture surface of 04Cr16Ni56 alloys under static loading of compact specimens in helium (a) and hydrogen (b) under pressure 30 MPa at 293 K.

### 3. Influence of Temperature on Hydrogen Embrittlement of the Alloys.

The strength of the alloy 05Cr19Ni55 significantly decreases in helium at temperatures higher than 873 K. This process is accompanied by a decrease in plasticity parameters for the alloy 05Cr19Ni55 at temperature 873 K and a significant increase in the relative elongation and reduction of area for specimens made of this alloy at temperatures 973...1073 K (Fig.5, curves 5, 6). At temperatures range 973...1073 K we observed a decrease in plasticity parameters for the alloy 04Cr16Ni56 (Fig.5, curves 7, 8).

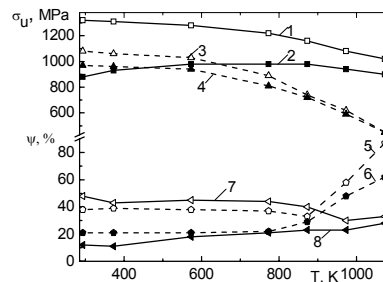


Figure 5. Temperature dependences of ultimate strength  $\sigma_u$  (1-4) and reduction of area  $\psi$  (5-8) of 04Cr16Ni56 (1, 2, 7, 8) and 05Cr19Ni55 (3, 4, 5, 6) alloys at helium (1, 3, 5, 7) and hydrogen (2, 4, 6, 8) under the pressure 30 MPa.

The drop of plasticity of the dispersion-hardening materials within the temperature range of intense phase transformations is caused by the localization of strains on the grain boundaries due to the intense redistribution of Ni, Ti, and Al in the boundary regions. Moreover, the increase in plasticity observed at higher temperatures is caused both by partial coagulation of hardening phases and possible dissolution of small amounts of finely divided precipitations [8]. In alloy 04Cr16Ni56 that contain higher amount of refractory elements (Table 1), the diffusion processes are decelerated and, therefore, the drop of strength is small and the temperature of plasticization is probably higher than 1073 K (Fig. 5, curves 1, 7).

The ultimate strength of alloy 04Cr16Ni56 is sensitive to hydrogen action (Fig. 5, curves 1, 2). At the same time  $\sigma_u$  of specimens made of alloy 05Cr19Ni55 decreases in hydrogen insignificantly (Fig. 5, curves 3, 4). The hydrogen effect on plasticity parameters  $\delta$  and  $\psi$  (Fig. 6), low-cycle durability  $N$  (Fig. 6) and plane-stress fracture toughness  $K_c$  (Fig. 7) of both alloys is essential in the temperature range 293...773 K and appreciable at all other temperatures. As temperature increases from 773 to 873 K the hydrogen effect on reduction of area of the alloy 05Cr19Ni55 specimens initially decrease and again increase at 973 and 1073 K (Fig. 5, curves 5, 6). That suggests that at 1073 K the hydrogen-induced processes of localization of strains and fracture (mainly intergranular) occur in this alloy so intensely that the coagulation of hardening phases is insufficient for the high-temperature plasticization observed in helium. This phenomenon we established earlier on dispersion-hardening austenitic steels [13].

The additional effect of preliminary hydrogenation on parameter of static growth resistance  $K_c$  for the alloy 05Cr19Ni55 is appreciable only at room temperature (Fig. 6, curves 3, 4, 6, 7). At 373 K the value of  $K_c$  for hydrogenated and non-hydrogenated specimens are almost equal, i.e., this temperature is sufficient for hydrogenation of dispersion-hardening nickel base alloys from the hydrogen atmosphere. For all loading modes, the degree and temperature interval of hydrogen degradation for alloy 04Cr16Ni56 is much larger than for alloy 05Cr19Ni55 (figs. 5-7).

The plane-strain condition required for the evaluation of  $K_{Ic}$  were fulfilled on compact tension specimens made of alloy 04Cr16Ni56 with a thickness of 20 mm at hydrogen pressure above 10 MPa in the temperature range 293...473 K. Fracture toughness  $K_c$  for alloy 05Cr19Ni55 was decreased at 293 K from  $116 \text{ MPa}\cdot\text{m}^{1/2}$  in helium to  $78 \text{ MPa}\cdot\text{m}^{1/2}$  in hydrogen under the pressure

30 MPa and to  $68 \text{ MPa}\cdot\text{m}^{1/2}$  in hydrogen under the pressure 30 MPa after preliminary high-temperature hydrogenation (with hydrogen concentration 19 ppm). The plane-strain conditions were not fulfilled at these two cases.

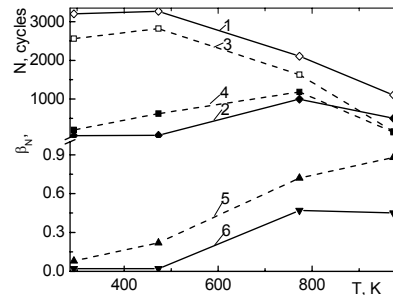


Figure 6. Temperature dependences of number cycles to failure  $N$  (1-4) ( $\varepsilon = 1,6\%$ ) and coefficients of hydrogen influence  $\beta_N = N_H/N_{He}$  (5, 6) on 04Cr16Ni56 (1, 2, 6) and 05Cr19Ni55 (3, 4, 5) alloys: 1, 3 – helium, 2, 4 – hydrogen under the pressure 30 MPa.

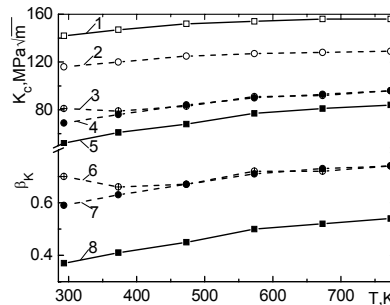


Figure 7. Temperature dependences of plane-stress fracture toughness  $K_c$  (1-5) and coefficients of hydrogen influence  $\beta_K = K_c^H/K_c^{He}$  (6-8) on 04Cr16Ni56Nb5Mo5TiAl (1, 5, 8) and 05Cr19Ni55Nb2Mo9Al (2-4, 6, 7) alloys: 1, 2 – helium, 2, 3, 6 – hydrogen under the pressure 30 MPa, 4, 7 – hydrogen under the pressure 30 MPa after preliminary hydrogenation (623 K, 35 MPa  $H_2$ , 10 h).

### Conclusions.

The parameters of loading and the modes of hydrogen action for which the mechanical characteristics of the investigated alloys are minimum at room temperature can be formulated as follows:

- strain rate  $V_{def} \leq 6.7 \cdot 10^{-5} \text{ s}^{-1}$  for tensile test and the strain amplitude  $\varepsilon = 1.6 \%$  under the conditions of low-cycle fatigue at hydrogen pressures above 10 MPa for the alloy 04Cr16Ni56 and hydrogen pressures above 15 MPa at concentration of preabsorbed hydrogen 19 wppm for the alloy 05Cr19Ni55;
- for static crack propagation at hydrogen pressure above 10 MPa for the alloy 04Cr16Ni56 and hydrogen pressure above 15 MPa at concentration of absorbed hydrogen 19 wppm for the alloy 05Cr19Ni55.

The plane-strain conditions required for the evaluation of  $K_{Ic}$  were fulfilled on compact tension specimens made of alloy 04Cr16Ni56 with thickness of 20 mm at hydrogen pressure above 10 MPa in the temperature range 293...473 K.

For all loading modes, the degree and temperature interval of hydrogen degradation for 04Cr16Ni56 alloy is much larger than for 05Cr19Ni55 alloy.

### References

- [1] Chandler W.I. and Walter R.I. Testing to determine the effect of high pressure hydrogen environment on the mechanical properties of metals, in: Hydrogen Embrittlement Testing,

- ASTM STP 543, Philadelphia, 1974, pp. 170–197.
- [2] N.R. Moody, F.A. Greulich, Hydrogen induced slip band fracture in Fe-Ni-Co superalloy. *Scr. Metallurgica*, 19 (1985) 1107-1116.
- [3] A. I. Balitkii, L.M. Ivaskevich, V.M. Mochulskiy. Temperature Dependences of Age-Hardening Austenitic Steels Mechanical Properties in Gaseous Hydrogen, in: Proceedings on CD ROM of the 12th International Conference on Fracture, Ottawa, Canada, July 12-17, 2009, edited by M. Elboujdaini, Ottawa: NRC, 2009, Paper No T19.001. 7 p.
- [4] Physicomechanical Institute: Development and Achievements [in Ukrainian], Lviv, 2001, 430 p.
- [5] A. I. Belogurov, V. S. Radchuk, M. A. Rudis, A. M. Sushkov, and V. I. Kholodnyi, Strength analysis of structural elements of hydrogen power-generating equipment, *Materials Science*, 40, (2004), No. 6, pp. 814—821.
- [6] B. A. Kolachev, Hydrogen Brittleness of Metals [in Russian]. *Metallurgiya*, Moscow, 1985.
- [7] V. I. Tkachev, L. M. Ivaskevich, V. I. Vitvitskii, Specific features of determination of the susceptibility of steels to hydrogen degradation. *Altern. Energ.*, 32 (2005). No. 12, 46-51.
- [8] C. T. Sims and W. C. Hagel (eds.). *The Superalloys*. Wiley, New York, 1972.
- [9] V. I. Tkachev, I. M. Levina, L. M. Ivaskevich, Distinctive features of hydrogen degradation of heat-resistant alloys based on nickel, *Materials Science*, 33 (1997), No. 4, 524-531.
- [10] W. F. Brown, J. E. Srawley. *Plane Strain Crack Toughness Testing of High Strength Metallic Materials*, ASTM Publ., No. 410, 1966.
- [11] LECO TCH 600 – Series (Nitrogen, Oxygen, Hydrogen Determination), LECO Corporation : MI, USA, 2003. 6 p.
- [12] H. R. Gray. Testing for hydrogen environment embrittlement: Experimental variables. In: *Hydrogen Embrittlement Testing*, ASTM STP 543, ASTM Baltimore, 1974, pp. 133-151.
- [13] V. I. Tkachev, L. M. Ivaskevich, V.M. Mochulskiy, Temperature dependences of mechanical properties of austenitic and martensitic steels in hydrogen, *Materials Science*, 45, (2007), No 5, 654-666